As seen from Table III, the total ligation ability (log β_2) of the μ-carbido dimer decreases along the following sequence: dication > cation > neutral > anion. This trend is not unexpected and is followed for a large number of other iron porphyrins.[28] This trend also predicts that there should be no interaction of py with $[((TPP)Fe)_2C]^{2-}$. This dianionic complex is isoelectronic with $((TPP)Fe)_2O$, which does not bind py under any conditions.

Great care must be taken in making comparisons between ligand binding properties of the μ-oxo, μ-nitrido, and μ-carbido dimers. One notable difference in these complexes (in addition to the overall oxidation state) is the out-of-plane distance of the iron atom. $((TPP)Fe)_2O$ has the most out-of-plane iron atom (0.50 Å),[29] while $((TPP)Fe)_2C$ has the smallest out-of-plane iron distance (0.26 Å).[14] $((TPP)Fe)_2N$ has the iron atom removed by 0.32 Å from the mean porphyrin plane,[3] which is closer to that of $((TPP)Fe)_2C$ than that of $((TPP)Fe)_2O$. However, it is clear that changes in iron out-of-plane distances will also occur upon the stepwise binding of the two axial pyridine ligands. Structural studies of mono- and bis(pyridine) adducts, when available, should help to clarify the magnitude of formation constants obtained in this study and might explain the reason for the favoring of a single ligand-binding reaction by $((TPP)Fe)_2C$.

Acknowledgment. The support of the National Institutes of Health is gratefully acknowledged (Grant GM 25172). We also acknowledge helpful discussions with Dr. Larry A. Bottomley.

Registry No. $((TPP)Fe)_2C$, 75249-87-5; $[((TPP)Fe)_2C(py)_2]^{2+}$, 92054-65-4; $[((TPP)Fe)_2C(py)_2]^{2+}$, 92054-66-5; $[((TPP)Fe)_2C]^-$, 83928-16-9; py, 110-86-1.

(29) Hoffman, A. B.; Collins, D. M.; Day, V. W.; Fleischer, E. B.; Srivastava, T. S.; Hoard, J. L. *J. Am. Chem. Soc.* **1972**, *94*, 3620.

Contribution from the Department of Chemistry, University of Houston, Houston, Texas 77004, Laboratoires de Chimie, LA au CNRS No. 321, Département de Recherche Fondamentale, Centre d'Etudes Nucléaires de Grenoble, F.38041 Grenoble Cedex, France, and Laboratoire d'Electrochimie et de Chimie Physique, ERA au CNRS No. 468, Université Louis Pasteur, F.67000 Strasbourg, France

Electrochemistry of Oxo- and Peroxotitanium(IV) Porphyrins. Mechanism of the Two-Electron Reduction of a η^2-Coordinated Peroxo Ligand

TADEUSZ MALINSKI,[1a,d] DANE CHANG,[1a] JEAN-MARC LATOUR,[1b] JEAN-CLAUDE MARCHON,*[1b] MAURICE GROSS,[1c] ALAIN GIRAUDEAU,[1c] and KARL M. KADISH*[1a]

Received April 26, 1984

The oxidation and reduction reactions of oxotitanium(IV) tetraphenylporphyrin, TiO(TPP), peroxotitanium(IV) tetraphenylporphyrin, $Ti(O_2)(TPP)$, and peroxotitanium(IV) octaethylporphyrin, $Ti(O_2)(OEP)$, in dichloromethane were investigated by electrochemical and spectroscopic techniques. Two one-electron oxidations and two one-electron reductions of the porphyrin ring were observed for TiO(TPP). Similar oxidations were found for $Ti(O_2)(TPP)$ and $Ti(O_2)(OEP)$. In addition, the peroxo complexes showed three reduction steps. The first reduction gives a porphyrin anion radical complex, which undergoes protonation by trace water followed by internal electron transfer to give a hydroperoxotitanium(III) porphyrin complex. The latter is then reduced at the porphyrin-ring system. Finally, internal transfer of two electrons cleaves the oxygen–oxygen bond of the coordinated hydroperoxide to give the oxotitanium(IV) porphyrin complex and hydroxide ion. The overall reaction is a two-electron reduction of the peroxo ligand in an ECEC mechanism. The oxotitanium(IV) complex that is obtained can be further reduced to the anion radical and the dianion of the porphyrin ring. Possible competing processes, which result in a substoichiometric reduction of the peroxo ligand, are surveyed.

Introduction

Studies of dioxygen complexes of transition-metal porphyrins are of intrinsic importance in providing a better understanding of the bonding and reactivity of the dioxygen ligand in biological systems.[2-4] The properties of synthetic cobalt(II)[5-7] and iron(II)[8,9] porphyrin oxygen carriers have been intensively investigated. Among first-row transition-metal complexes, dioxygen adducts have also been obtained with chromium(II),[10] manganese(II),[11,12] and titanium(III) porphyrins.[13]

Recently, some of the present investigators (University of Houston) reported electrochemical studies of the diperoxomolybdenum(VI) porphyrin complex, $Mo^{VI}(O_2)_2(TmTP)$[14] (where TmTP is 5,10,15,20-tetra-*m*-tolylporphinato). It was shown that reduction occurred at the central metal and not at the porphyrin ring. This provided the first example where a peroxo-bound metalloporphyrin could be reduced at the central metal without affecting the nature of the metal–oxygen bond. This inertness was not observed by some of the present authors (C.E.N. Grenoble) in preliminary studies of the peroxotitanium(IV) porphyrin complex, $Ti^{IV}(O_2)(TPP)$ (where TPP is 5,10,15,20-tetraphenylporphinato). It was reported[15] that $Ti(O_2)(TPP)$ is electrochemically reduced in a two-electron irreversible process to the corresponding oxo complex,

(1) (a) University of Houston. (b) Centre d'Etudes Nucléaires de Grenoble. (c) Université Louis Pasteur. (d) Present address: Department of Chemistry, Oakland University, Rochester, MI 48063.
(2) Basolo, F.; Hoffman, B. M.; Ibers, J. A. *Acc. Chem. Res.* **1975**, *8*, 384-392 and references therein.
(3) Collman, J. P. *Acc. Chem. Res.* **1977**, *10*, 265-272.
(4) Jones, R. D.; Summerville, D. A.; Basolo, F. *Chem. Rev.* **1978**, *78*, 139-179.
(5) Walker, F. A. *J. Am. Chem. Soc.* **1970**, *92*, 4235-4244.
(6) Stynes, D. V.; Stynes, H. C.; James, B. R.; Ibers, J. A. *J. Am. Chem. Soc.* **1973**, *95*, 1796-1801.
(7) Hoffman, B. M.; Petering, D. H. *Proc. Natl. Acad. Sci. U.S.A.* **1970**, *67*, 637-643.
(8) Collman, J. P.; Gagne, R. R.; Reed, C. A.; Halbert, T. R.; Lang, G.; Robinson, W. T. *J. Am. Chem. Soc.* **1975**, *97*, 1427-1439.
(9) James, B. R. In "The Porphyrins"; Dolphin, D., Ed.; Academic Press: New York, 1978; Vol. 5.
(10) Cheung, S. T.; Grimes, C. J.; Wong, J.; Reed, C. A. *J. Am. Chem. Soc.* **1976**, *98*, 5028-5030.
(11) Gonzales, B.; Kouba, J.; Yee, S.; Reed, C. A.; Kirner, J.; Scheidt, W. R. *J. Am. Chem. Soc.* **1975**, *97*, 3247-3249.
(12) Hoffmann, B. M.; Wechsler, C. J.; Basolo, F. *J. Am. Chem. Soc.* **1976**, *98*, 5473-5482.
(13) Latour, J.-M.; Marchon, J.-C.; Nakajima, M. *J. Am. Chem. Soc.* **1979**, *101*, 3974-3976.
(14) Kadish, K. M.; Chang, D.; Malinski, T.; Ledon, H. *Inorg. Chem.* **1983**, *22*, 3490-3492.
(15) Guilard, R.; Latour, J.-M.; Lecomte, C.; Marchon, J.-C.; Protas, J.; Ripoll, D. *Inorg. Chem.* **1978**, 17, 1225-1235.

0020-1669/84/1323-3947$01.50/0

Table I. Half-Wave Potentials (V vs. SCE) for the Redox Reactions of Titanium(IV) Porphyrins in CH_2Cl_2 (0.1 M TBAP) (Scan Rate 0.1 V/s)

	redn waves				oxidn waves[a]				
porphyrin	I	II	III	III′	IV	V	VI	VII	VIII
TiO(TPP)		−1.04	−1.43					1.20	1.42
$Ti(O_2)$(TPP)	−0.97[b] (−0.91)[c] −1.16[d]	−1.04	−1.43 −1.55[d]	−1.35	−0.44	−0.03	0.65	1.19	1.32
$Ti(O_2)$(OEP)	−1.18[b] (−1.11)[c] −1.25[e]	−1.23	−1.76 −1.80[e]		−0.55	−0.12	0.56	1.04	1.35

[a] Waves IV–VI were not observed on initial reductive scans and were only present on the reverse (oxidative) potential scan after sweeping cathodically to −0.95 V or greater at a scan rate >0.1 V/s (see dotted line, Figure 5). [b] Cathodic peak potential. [c] Half-wave potential determined by dc polarography. [d] Half-wave potential obtained at −60 °C. [e] Half-wave potential at −20 °C.

TiO(TPP). The nature of the electrolysis product suggested that reduction occurred at the axial peroxide ligand, and the overall process was schematically described by eq 1 and 2.

$$Ti^{IV}(O_2)(TPP) + 2e^- \rightarrow [Ti^{IV}(O)_2(TPP)]^{2-} \quad (1)$$

$$[Ti^{IV}(O)_2(TPP)]^{2-} + H_2O \rightarrow Ti^{IV}O(TPP) + 2HO^- \quad (2)$$

In order to elucidate the mechanism of the reductive cleavage of the O–O bond in this system, we have undertaken detailed chemical, electrochemical, spectroelectrochemical, and ESR studies of $Ti(O_2)$(TPP) and $Ti(O_2)$(OEP) oxidation/reduction. Results of this study are presented in this paper.

Experimental Section

Oxotitanium(IV) tetraphenylporphyrin, TiO(TPP),[16] peroxotitanium(IV) tetraphenylporphyrin, $Ti(O_2)$(TPP),[15] and peroxotitanium(IV) octaethylporphyrin, $Ti(O_2)$(OEP)[15] were synthesized and purified by previously reported methods. Methylene chloride, CH_2Cl_2, was purchased from Fisher Scientific Co. as technical grade and was twice distilled from P_2O_5 before use. The supporting electrolyte, tetrabutylammonium perchlorate (TBAP), was recrystallized from ethyl acetate/hexane and dried in vacuo prior to use.

Cyclic voltammetric measurements were made by using a conventional three-electrode configuration and the combination of a Princeton Applied Research (PAR) Model 174A polarographic analyzer and a Model 175 Universal Programmer. A platinum button served as a working electrode and a platinum wire as a counterelectrode for conventional cyclic voltammetric measurements. A saturated calomel electrode (SCE), which was separated from the bulk of the solution by a fritted glass disk, was used as the reference electrode. Current–voltage curves were recorded on a Houston Instruments Omnigraphic X-Y recorder at scan rates from 0.05 to 0.30 V/s and on a Tektronix 5111 storage oscilloscope using a Tektronix C-5A oscilloscope camera at scan rates from 0.5 to 20 V/s.

Bulk-scale controlled-potential coulometry and controlled-potential electrolysis were done with a PAR Model 173 potentiostat to control the potential. Integration of the current–time curve was achieved by means of a PAR Model 179 integrator. A three-electrode configuration was used, consisting of a Pt-wire-mesh working electrode, a Pt-wire counterelectrode separated from the main solution by a glass frit, and an SCE as the reference electrode. Deaeration and stirring were achieved by means of a stream of high-purity nitrogen, which was passed throughout the solution. Spectroelectrochemistry was performed in a bulk cell as well as in a thin-layer cell. The bulk cell followed the design of Fajer et al.[17] and had an optical path length of 0.19 cm. The thin-layer cell has a 1000-lpi gold minigrid working electrode sandwiched between two glass slides and a platinum-gauze electrode. In both cases, the SCE was separated from the test solution by a fritted bridge containing supporting electrolyte and solvent. Both spectrophotometric cells were coupled with a Tracor Northern 1710 optical spectrometer-multichannel analyzer to obtain time-resolved spectra. The spectra result from the signal averaging of 100 5-ms spectral acquisitions. Each acquisition represents a single spectrum from 325 to 950 nm, simultaneously recorded by a double-array detector with a resolution of 1.2 nm/channel. ESR spectra were recorded on an IBM Model ER 100D spectrometer, equipped with an ER 040-X microwave bridge and an ER 080 power supply, or on a Varian Model E-104 spectrometer. Low-temperature ESR spectral measurements were achieved with a Varian variable-temperature controller, which monitored the temperature from 0 to −150 °C. The g values were measured relative to diphenylpicrylhydrazyl (DPPH) ($g = 2.0036 \pm 0.0003$).

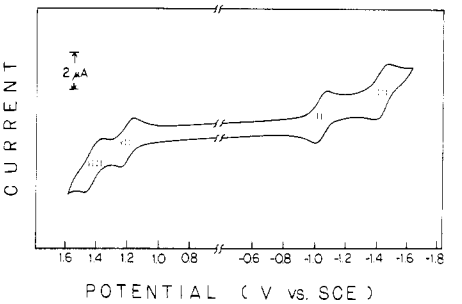

Figure 1. Cyclic voltammogram of TiO(TPP) in CH_2Cl_2 (0.1 M TBAP) (scan rate 0.1 V/s).

Chemical reduction of TiO(TPP) and $Ti(O_2)$(TPP) was done in a Jaram inert-atmosphere glovebox under argon containing less than 1 ppm of O_2 and H_2O. Tetrahydrofuran (THF) was distilled from a solution of sodium benzophenone ketyl in the glovebox. A stock solution was prepared shortly before each reduction experiment by dissolving 34 mg of sodium (1.5 mmol) in a solution containing 267 mg of anthracene (1.5 mmol) in 10 mL of THF. In a typical experiment, TiO(TPP) (20 mg, 3×10^{-2} mmol) was dissolved in 20 mL of THF. Sodium anthracenide stock solution (100 μL, 0.5 equiv) and solid TBAP (200 mg 8.3×10^{-1} mmol) were then added. An aliquot of the resulting solution was diluted 10-fold to run the ESR and visible spectra; this was conveniently done by adding 10 drops of solution to 90 drops of pure THF. Spectra were run again in the same way after addition of methanol (10 drops).

Results and Discussion

Reduction of TiO(TPP). Figure 1 illustrates a typical cyclic voltammogram of TiO(TPP) in CH_2Cl_2 (0.1 M TBAP). As seen in this figure, two reversible reduction processes occur at −1.04 and −1.43 V vs. SCE (labeled II and III). Half-wave potentials of these redox couples are listed in Table I. The currents observed for the two reductions are equal in height, the peak separation $E_{pa} - E_{pc} = 60 \pm 5$ mV (for a scan rate $v = 0.1$ V/s), and a constant value of $i_p/v^{1/2}$ was obtained. This indicated that one electron is reversibly transferred in each step and that both electrode processes are diffusion controlled.[18]

The number of electrons transferred in each step was confirmed by controlled-potential electrolysis, which was carried out at potentials 200 mV more negative than the first and second reduction potentials. The first reduction involved a one-electron addition as the solution color changed from pink to yellow-green. This reduction was reversible at electrolysis times less than 5 min as evidenced by the fact that reoxidation

(16) Fournari, P.; Guilard, R.; Fontesse, M.; Latour, J.-M.; Marchon, J.-C. *J. Organomet. Chem.* **1976**, *110*, 205–217.
(17) Fajer, J.; Borg, D. C.; Forman, A.; Dolphin, D.; Felton, R. H. *J. Am. Chem. Soc.* **1970**, *92*, 3451–3459.
(18) Nicholson, R. S.; Shain, I. *Anal. Chem.* **1964**, *36*, 706–723.

Table II. Absorption Maxima (nm) and Molar Absorptivities (ϵ) of Oxidized and Reduced Titanium(IV) Complexes in CH_2Cl_2 (0.1 M TBAP)[a]

porphyrin	λ_{max}, nm ($10^4\epsilon$)									
	neutral		Red(1)		Red(2)		Ox(1)		Ox(2)	
TiO(TPP)	422 (29.3)	511 (0.35)	422 (22.8)		423 (7.06)		422 (8.87)	454 (sh)	422 (4.05)	471 (sh)
	551 (1.81)	589 (0.39)	551 (1.45)	589 (0.59)		631 (1.03)	808 (1.19)	890 (1.45)	505 (3.18)	593 (1.08)
			631 (0.70)						644 (1.04)	
$Ti(O_2)$(TPP)	423 (19.6)	533 (sh)	423 (20.1)	450 (7.35)	423 (19.69)	511 (0.68)	423 (19.23)	460 (sh)	428 (9.53)	460 (8.96)
	548 (1.51)	592 (0.36)	506 (0.60)	549 (1.23)	551 (1.56)	589 (0.77)	533 (sh)	548 (0.88)	730 (0.44)	809 (1.13)
			589 (0.51)	631 (0.40)	631 (0.70)	645 (0.81)	809 (0.72)	895 (1.01)		
			691 (0.62)	754 (1.21)						
$Ti(O_2)$(OEP)	405 (17.52)	496 (sh)	404 (18.6)	535 (1.40)	404 (18.55)	535 (1.45)	391 (13.82)	535 (0.58)	391 (6.36)	481 (1.20)
	535 (1.08)	572 (1.47)	573 (2.06)		573 (2.10)	632 (0.18)	568 (0.55)	630 (0.43)	553 (0.45)	582 (0.43)
							668 (0.27)		667 (0.83)	

[a] sh = shoulder.

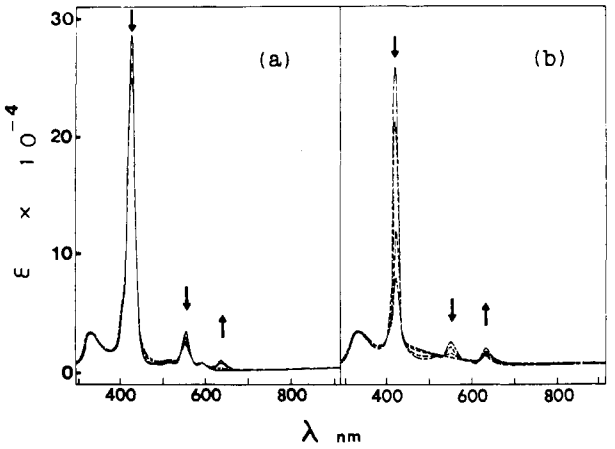

Figure 2. Time-resolved electronic absorption spectra for reduced TiO(TPP) in CH_2Cl_2 (0.1 M TBAP). Spectra were taken (a) during the first reduction at an applied potential of −1.24 V and (b) during the second reduction at −1.63 V.

could be accomplished at −0.7 V with the abstraction of one electron, while producing the original pink color. The second one-electron reduction of TiO(TPP) produced a green solution and was irreversible on the controlled-potential electrolysis time scale.

Spectral changes recorded during stepwise exhaustive reduction of TiO(TPP) are shown in Figure 2, and values of wavelengths and molar absorptivities are listed in Table II. During the first step of electrolysis, the Soret peak at 422 nm as well as the band at 551 nm decreased slightly and a new peak at 631 nm appeared (Figure 2a). This spectrum can be assigned as due to the porphyrin anion radical $[TiO(TPP\cdot)]^-$. The final spectrum obtained after the second reduction of TiO(TPP) has a significantly decreased Soret band at approximately the same wavelength as the starting complex (Figure 2b). This spectrum can be assigned to the porphyrin dianion $[TiO(TPP)]^{2-}$.

Before electrolysis no ESR was observed. The ESR spectrum of the solution obtained after the first reduction step showed both room-temperature and low-temperature isotropic signals, with g values ranging from 2.005 to 2.007. These are characteristic of anion radicals.[19] No ESR signal was observed after the second reduction.

On the basis of the above electrochemical and spectral data, the first and second reduction of TiO(TPP) may be described by eq 3 and 4 where the Roman numerals II and III correspond to the reversible reductions shown in Figure 1. Similar

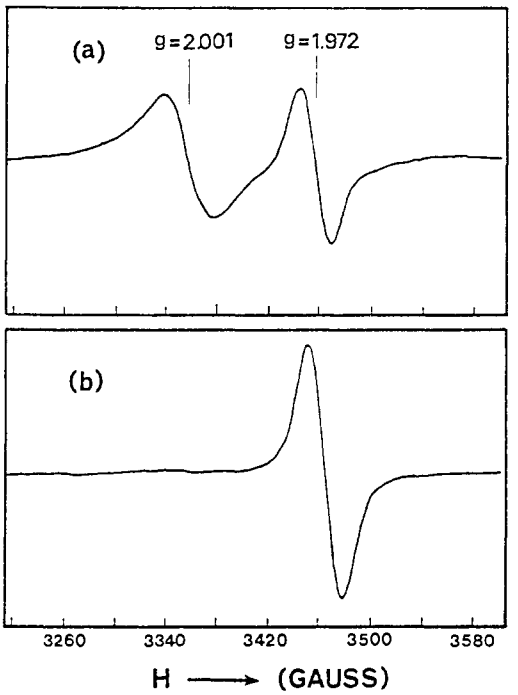

Figure 3. Room-temperature ESR spectra of TiO(TPP) in THF (4 × 10^{-3} M TBAP), obtained after addition of 0.5 equiv of sodium anthracenide and (a) aging 4–5 days and (b) adding excess deoxygenated methanol. Conditions of ESR spectroscopy: microwave power, 10 mV; modulation, 0.5 G; gain, 6.3 × 10^2 (for (a)) and 3.2 × 10^2 (for (b)); frequency, 9.52 GHz; scan, 400 G.

ring reductions have been described for TiO(OEP) in Me_2SO.[20]

$$Ti^{IV}O(TPP) + e^- \overset{II}{\rightleftharpoons} [Ti^{IV}O(TPP\cdot)]^- \quad (3)$$

$$[Ti^{IV}O(TPP\cdot)]^- + e^- \overset{III}{\rightleftharpoons} [Ti^{IV}O(TPP)]^{2-} \quad (4)$$

In order to obtain more information on any chemical reactions that may follow the first reduction of TiO(TPP), the porphyrin anion radical $[TiO(TPP\cdot)]^-$ was generated by chemical reduction in strictly anhydrous and deoxygenated solutions in a glovebox under argon (O_2, H_2O < 1 ppm). Addition of 0.5 equiv of sodium anthracenide in tetrahydrofuran to a solution of TiO(TPP) in the same solvent containing 4 × 10^{-2} M TBAP gave rise to an intense ESR signal at g = 2.001, while a peak appeared at 631 nm in the visible spectrum of the solution. The intensity of this ESR signal decreased very slowly with time, while a new signal appeared at g = 1.972 at the expense of the former. The spectrum obtained after 4–5 days is shown in Figure 3a. At this stage, addition of a few equivalents of deoxygenated methanol immediately converted the remaining g = 2.001 species to the g = 1.972

(19) Fajer, J.; Davis, M. S. In "The Porphyrins"; Dolphin, D.; Ed.; Academic Press: New York, 1979; Vol. 4.
(20) Fuhrhop, J.-H.; Kadish, K. M.; Davis, D. G. *J. Am. Chem. Soc.* **1973**, *95*, 5140–5147.

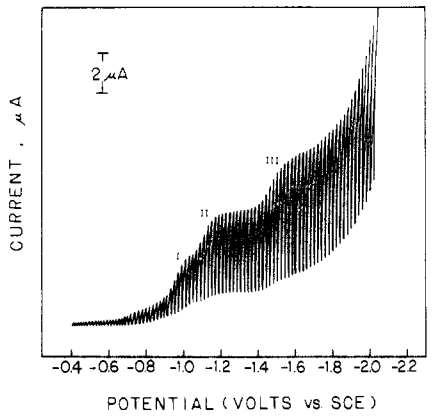

Figure 4. Dc polarogram of 1 mM $Ti(O_2)(TPP)$ in CH_2Cl_2 (0.1 M TBAP) solution.

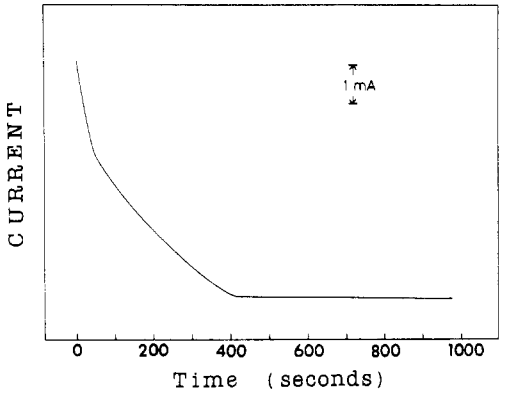

Figure 5. Current–time curve obtained during controlled-potential electrolysis of $Ti(O_2)(TPP)$ at −0.98 V in CH_2Cl_2 (0.1 M TBAP).

species in a quantitative manner (Figure 3b).

Five-coordinate titanium(III) tetraphenylporphyrin complexes exhibit isotropic ESR signals at g = 1.972–1.977 at room temperature in dichloromethane or toluene solution.[21] Thus, it can safely be assumed that reaction of the porphyrin anion radical complex $[TiO(TPP\cdot)]^-$ with trace water slowly released from the glassware, or with methanol, leads to a five-coordinate titanium(III) porphyrin complex by internal electron transfer according to reaction 5, where R = H or CH_3.

$$[Ti^{IV}O(TPP\cdot)]^- + ROH \rightarrow Ti^{III}(OH)(TPP) + RO^- \quad (5)$$

This reaction can be described as a proton transfer from water or methanol to the oxo ligand, which weakens the Ti^{IV}–O bond and makes possible the transfer of an electron from the porphyrin ring to the titanium(IV) center.

Reduction of $Ti(O_2)(TPP)$. A typical dc polarogram for the reduction of $Ti(O_2)(TPP)$ is shown in Figure 4. Three well-defined reductions are obtained at $E_{1/2}$ = −0.91, −1.04, and −1,43 V. These waves have approximately equal diffusion-limiting currents and an $E_{1/4} - E_{3/4} = 60 \pm 5$ mV. This slope is diagnostic for a diffusion-controlled one-electron transfer in each step.[22] However, this could not be confirmed by coulometric measurements in macroscale electrolysis. When coulometry was carried out at an applied potential of −0.98 V, 2.2 + 0.05 faradays were obtained, in fair agreement with the results of the preliminary study.[15] The current–time curve for this electrolysis process is shown in Figure 5. As can be seen in this figure, the current–time curve is not straightforward. Analysis of the curve indicates that initial

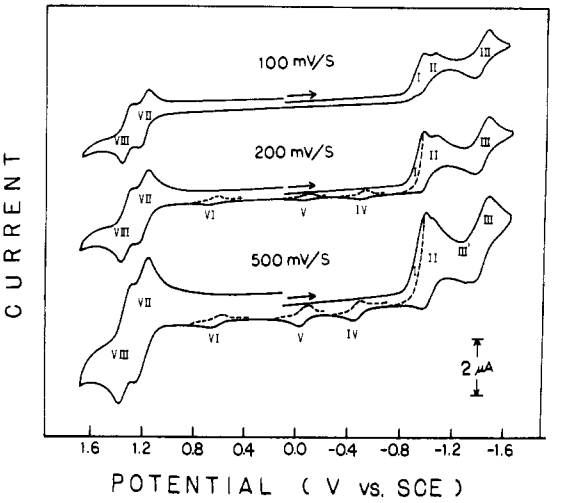

Figure 6. Cyclic voltammograms of 1 mM $Ti(O_2)(TPP)$ in CH_2Cl_2 (0.1 M TBAP) solution at various potential scan rates.

reduction is followed by a chemical reaction and that the product of the chemical reaction undergoes further reduction. When the electrode potential was shifted to −1.20 V (second reduction step), no current was detected.

In order to resolve this ambiguity in the polarographic and coulometric results and to make the assignment of waves I–III, the reduction and reoxidation of $Ti(O_2)(TPP)$ were investigated by the technique of cyclic voltammetry as a function of scan rate and temperature. Typical cyclic voltammograms of $Ti(O_2)(TPP)$ obtained in CH_2Cl_2 at 22 °C at different scan rates are shown in Figure 6. In the range of potentials between +0.3 and −1.6 V vs. SCE, three reduction peaks were obtained with continuous scan. The first process at E_{pc} = −0.97 V has a slope $E_p - E_{p/2}$ = 60 mV. The peak potential was shifted negatively with an increase in scan rate, and there was no observable reoxidation wave for scan rates up to 500 mV/s. The two subsequent processes remained reversible (at a scan rate of 100 mV/s) with half-wave potentials identical with those observed in dc polarography (see Table I). At scan rates higher than 3 V/s a significant decrease in the currents of the cathodic peak II as well as a positive shift of the anodic peak II was observed. At a scan rate of 10 V/s two quasi-reversible couples were obtained, one at $E_{1/2}$ = −0.92 V and the second at $E_{1/2}$ = −1.42 V.

At scan rates higher than 0.20 V/s reversal of the potential scan at either −0.96, −1.20, or −1.60 V yielded new oxidation peaks (labeled IV–VI in Figure 6) at $E_{1/2}$ = −0.44, −0.03, and 0.65 V. All of these processes were either reversible or quasi-reversible (at high potential scan rate), and the observed currents were approximately equal in height. These peaks were not observed upon initial reduction scans of $Ti(O_2)(TPP)$ solutions nor were they observed if the time between the switching potential at E = −0.99 V and the oxidation potential of peak IV was longer than 4 s. Thus, it is clear from this data and from Figure 6 that peaks IV–VI are due either to oxidation processes involving the products of the first reduction (peak I) or to oxidation processes involving a decomposition product(s) of the singly reduced species.

The half-wave potential for peak IV is −0.44 V and is close to the potential of −0.45 V reported for the oxidation Ti(III) to Ti(IV)[23] according to reaction 6. This suggests that the

$$[Ti^{III}F_2(TPP)]^- \rightleftharpoons Ti^{IV}F_2(TPP) + e^- \quad (6)$$

process occurring at −0.44 V (peak IV) may be assigned to

(21) Latour, J.-M. Thèse de Docteur ès-Sciences Physiques, Université de Grenoble, 1980.
(22) Meites, L. In "Polarographic Techniques"; Interscience: New York, 1965.
(23) Nakajima, M.; Latour, J.-M.; Marchon, J.-C. *J. Chem. Soc., Chem. Commun.* **1977**, 763–764.

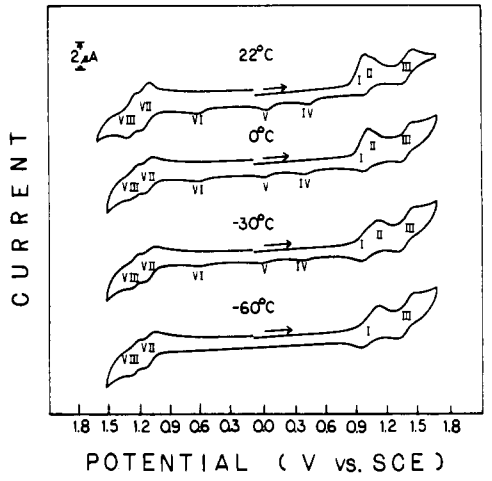

Figure 7. Cyclic voltammograms of 1 mM $Ti(O_2)(TPP)$ in CH_2Cl_2 (0.1 M TBAP) solution at various temperatures.

the oxidation of a six-coordinate titanium(III) porphyrin complex as shown in reaction 7. Waves V and VI do not correspond to any known reactions of Ti(III) or Ti(IV) porphyrins with different axial ligands.

$$[Ti^{III}(X)(Y)(TPP)]^- \rightleftharpoons Ti^{IV}(X)(Y)(TPP) + e^- \quad (7)$$

Typical cyclic voltammograms of $Ti(O_2)(TPP)$ obtained as a function of temperature are shown in Figure 7. As the temperature was decreased from 22 °C, a significant decrease of currents for the cathodic peak II were observed. At −60 °C this peak completely disappeared, and the cathodic peak I was shifted to a more negative potential. At the same time, the anodic peak II was shifted to a more positive potential, so that it eventually merged with the couple involving the cathodic peak I. At a temperature of −60 °C only two reversible reduction couples were observed. These were at $E_{1/2}$ = −1.16 and −1.55 V. The same change in current–voltage curves was observed at high potential scan rates at 22 °C and yields additional confirmation that an ECE or ECEC mechanism is involved in the first reduction step.

In order to determine the site of reduction (π-ring system, metal center, or the peroxo group) the products of controlled-potential electrolysis were investigated by ESR and electronic absorption spectroscopy. Before electrolysis, no ESR signal was observed for $Ti(O_2)(TPP)$. However, after 50 s of electrolysis at −0.98 V, an isotropic ESR signal (g = 2.004) was obtained as shown in Figure 8a. This value is clearly indicative of a π-anion radical,[17] which would be $[Ti^{IV}(O_2)(TPP\cdot)]^-$. When electrolysis was continued for longer than 50 s, the spectrum showed an additional species that was also an anion radical (Figure 8b). An identical signal with g = 2.005 was obtained after the first reduction of $Ti^{IV}O(TPP)$ at −1.24 V. This suggests that partial overlap of waves I and II makes it difficult to carry out a controlled-potential electrolysis on the plateau of wave I without generating at the same time a small amount of $[TiO(TPP\cdot)]^-$, which is the reduction product associated with wave II.

The electronic absorption spectra associated with each controlled-potential reduction step of $Ti(O_2)(TPP)$ are shown in Figure 9 and the molar absorptivities of the major peaks summarized in Table II. During the first 50 s of electrolysis on the plateau of wave I (at −0.98 V), the Soret peak slightly increased and the α band slightly decreased in intensity (Figure 9a). At the same time new peaks appeared at 450, 631, 691, and 754 nm. Spectral absorption peaks in the range between 590 and 800 nm suggest radical anion formation,[24] and this

(24) Fuhrhop, J. H. *Struct. Bonding (Berlin)* **1974**, *18*, 1–67.

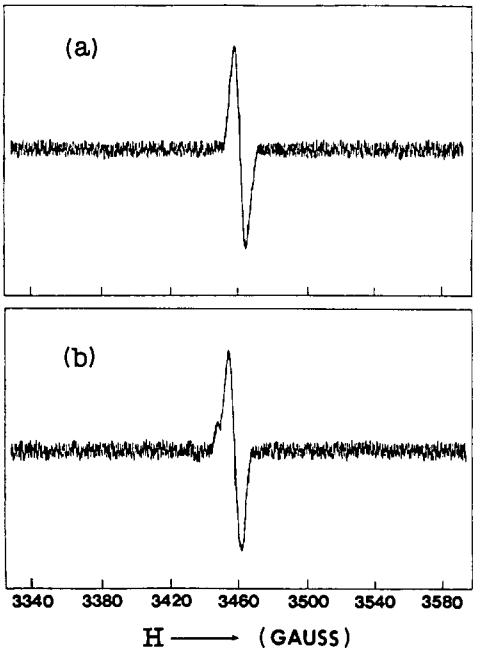

Figure 8. Room-temperature ESR spectra of $Ti(O_2)(TPP)$ in CH_2Cl_2 (0.1 M TBAP) obtained after (a) 50 s and (b) 300 s of electrolysis at −0.98 V vs. SCE.

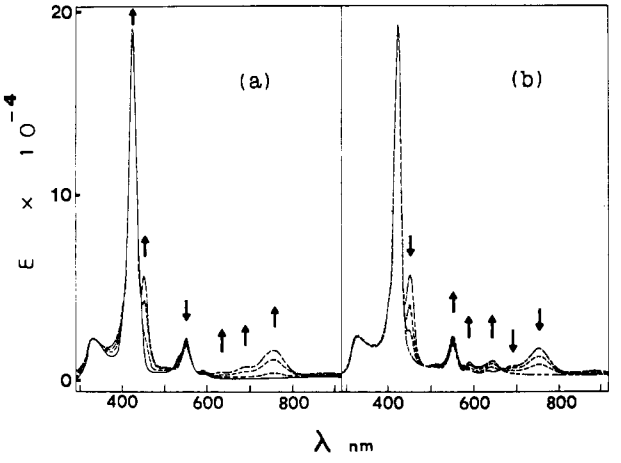

Figure 9. Time-resolved electronic absorption spectra for the reduction of $Ti(O_2)(TPP)$ in CH_2Cl_2 (0.1 M TBAP) at −0.98 V vs SCE (2-mm cell): (a) between 0 and 50 s electrolysis time; (b) between 50 and 300 s electrolysis time.

was confirmed by ESR spectroscopy. However, a radical anion was not the only product of the first reduction step, as can be seen by the cyclic voltammogram in Figure 6 (where oxidation peaks IV–VI are found). The absorption peak at 450 nm in Figure 9 can be assigned as a Soret peak of the $[Ti(O_2)(TPP\cdot)]^-$ radical or alternatively the Soret peak of a six-coordinate titanium(III) porphyrin complex. The Soret peak for $[Ti^{III}F_2(TPP)]^-$ occurs at 439 nm.[21]

When the electrolysis was carried out for longer than 50 s at −0.98 V, the peak at 450 nm as well as the peaks at 691 and 754 nm decreased and finally disappeared (Figure 9b). At the same time, peaks at 591 and 631 nm, which are characteristic of $[TiO(TPP\cdot)]^-$, increased. (See Figure 2a for $[TiO(TPP\cdot)]^-$ spectra.) A new peak also appeared at 645 nm. These wavelengths and values of molar absorptivities are included in Table II. On the basis of this spectral data, the final bulk electrolysis product at longer times can be assigned as the $[TiO(TPP\cdot)]^-$ anion radical. When the potential was switched from −0.98 to −1.24 V, no additional current was detected. This again indicates that the potential distribution at the electrode–solution interface encompasses both wave I

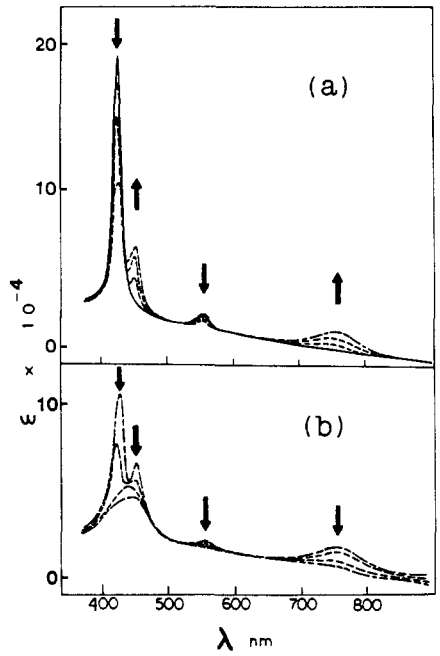

Figure 10. Thin-layer electronic absorption spectra obtained during reduction of $Ti(O_2)(TPP)$ in CH_2Cl_2 (0.1 M TBAP) at (a) −1.30 V and (b) −1.65 V.

and wave II, which are very close to each other, and that therefore the reduction product associated with wave II is formed when the potential is apparently fixed on wave I. This was confirmed by applying a potential directly on the plateau of wave II with a fresh solution. Under this condition (electrolysis at −1.24 V) a spectrum identical with that observed between 50 and 300 s of electrolysis at −0.98 V was obtained (see Figure 9b). Finally, macroelectrolysis of $Ti(O_2)(TPP)$ at −1.64 V gave a spectrum similar to that observed for the second reduction of TiO(TPP), i.e., the spectrum assigned to $[TiO(TPP)]^{2-}$ (see Figure 2b and Table II).

Thin-layer spectra were also obtained for the reduction of $Ti(O_2)(TPP)$. The spectrum obtained during the first reduction at −0.98 V was similar to that obtained during the first 50 s of the macroelectrolysis in a 2-mm cell (Figure 10a). However, in thin-layer spectroelectrochemistry, no change in the spectrum attributable to the $[TiO(TPP\cdot)]^-$ radical anion was observed up to a potential of −1.30 V. A major change of the $[Ti(O_2)(TPP\cdot)]^-$ spectrum was observed in the potential range −1.3 to −1.7 V, but the final obtained spectrum (Figure 10b) was different from that for $[TiO(TPP)]^{2-}$. This spectrum, which shows significant Soret and Q-band breakdown, can be assigned to the dianion $[Ti(O_2)(TPP)]^{2-}$.

Chemical reduction of $Ti(O_2)(TPP)$ by sodium anthracenide in anhydrous THF solution was also carried out in an inert-atmosphere glovebox. Addition of 1 equiv of reductant gave rise to an intense ESR signal at $g = 2.003$ that was assigned to the anion radical complex $[Ti(O_2)(TPP\cdot)]^-$. This signal decayed slowly and disappeared in about 24 h. On the other hand, addition of a few equivalents of methanol to a freshly prepared $[Ti(O_2)(TPP\cdot)]^-$ solution led to the rapid disappearance of the $g = 2.003$ signal, and no new signal appeared in the ESR spectrum. The visible spectrum of the final solution was similar to that of TiO(TPP). Finally, addition of 2 equiv of sodium anthracenide to $Ti(O_2)(TPP)$ gave an ESR-silent solution with a visible spectrum identical with that of TiO(TPP).

Thus, on the basis of electronic absorption spectra, ESR, and redox potentials, the first reduction of $Ti(O_2)(TPP)$ may be postulated to occur as shown in reaction 8. At low temperatures, the $[Ti^{IV}(O_2)(TPP\cdot)]^-$ radical is stable and reaction 8 is reversible. However, at temperatures higher than −60 °C, the $[Ti^{IV}(O_2)(TPP\cdot)]^-$ radical may undergo further reactions according to eq 8–11. By analogy with the protonation re-

$$Ti^{IV}(O_2)(TPP) + e^- \rightleftharpoons [Ti^{IV}(O_2)(TPP\cdot)]^- \quad (8)$$

$$[Ti^{IV}(O_2)(TPP\cdot)]^- + H_2O \rightarrow Ti^{III}(OOH)(TPP) + HO^- \quad (9)$$

$$Ti^{III}(OOH)(TPP) + e^- \rightleftharpoons [Ti^{III}(OOH)(TPP\cdot)]^- \quad (10)$$

$$[Ti^{III}(OOH)(TPP\cdot)]^- \rightarrow Ti^{IV}O(TPP) + HO^- \quad (11)$$

action described in eq 5 for $[Ti^{IV}O(TPP\cdot)]^-$, it can be safely assumed that proton transfer to the η^2-peroxo ligand of $[Ti^{IV}(O_2)(TPP\cdot)]^-$ weakens the titanium–peroxo bonding system and makes possible an internal electron transfer leading to the η^1-hydroperoxotitanium(III) porphyrin complex (reaction 9). The latter species is reasonably thought to be easier to reduce than $Ti(O_2)(TPP)$; therefore, this species can accept a second electron, either from the cathode (reaction 10) or, if reduction has been done by sodium anthracenide, from another $[Ti^{IV}(O_2)(TPP\cdot)]^-$ complex according to reaction 12.

$$Ti^{III}(OOH)(TPP) + [Ti^{IV}(O_2)(TPP\cdot)]^- \rightarrow [Ti^{III}(OOH)(TPP\cdot)]^- + Ti^{IV}(O_2)(TPP) \quad (12)$$

Reductive cleavage of the O–O bond of the hydroperoxo ligand can take place after this second electron has been stored in the porphyrin. This occurs by internal transfer of two electrons to the axial ligand followed by liberation of hydroxide ion according to reaction 11.

This proposed mechanism deserves a few comments. First, the initially formed anion radical complex, $[Ti(O_2)(TPP\cdot)]^-$, is a very unusual species: it contains in the same molecular framework a two-electron oxidant (the peroxo group) and a strong one-electron reductant (the porphyrin anion radical). However, these sites cannot interact readily with each other as the one-electron reduction of peroxide is energetically unfavorable, and the complex is stable enough for spectroscopic characterization in anhydrous solution. Reaction with a proton donor destroys this fragile equilibrium, however, by providing a pathway for the two-electron reduction of the coordinated peroxide. A key second feature of this mechanism is the possibility of shuttling electrons between the porphyrin ring and the titanium center and between the porphyrin ring and the axial peroxide ligand via the titanium atom, until two electrons are available for the reductive cleavage of the O–O bond of the coordinated peroxide.[25]

The overall reaction occurring in step I is a two-electron reduction of $Ti(O_2)(TPP)$ according to reaction 13. This is

$$Ti^{IV}(O_2)(TPP) + 2e^- + H_2O \rightarrow Ti^{IV}O(TPP) + 2HO^- \quad (13)$$

in fair agreement with the observed coulometry of 2.2 faradays at −0.98 V. This number, however, is an overall value for the first two reduction steps, which is due to the proximity of waves I and II as already noted above. It appears therefore that the two-electron reduction of the peroxo ligand occurs only to a

(25) An alternative mechanism for the two-electron reductive cleavage of the hydroperoxo complex generated by reaction 9 is as follows:

$$Ti^{III}(OOH)(TPP) \rightarrow [Ti^{IV}O(TPP\cdot)]^+ + HO^-$$

$$[Ti^{IV}O(TPP\cdot)]^+ + e^- \rightleftharpoons Ti^{IV}O(TPP)$$

In the first step, a two-electron reductive cleavage of the coordinated hydroperoxide is obtained by redox assistance of the porphyrin to the titanium(III) center. This would generate the cation radical complex, $[TiO(TPP\cdot)]^+$, which easily reduces to TiO(TPP) in a following step. Such a mechanism is reasonably thought to be inoperative in the present experimental conditions, as it is energetically more demanding to abstract an electron from the porphyrin HOMO (+1.20 V; vide infra) than from a cathode at an applied potential of −0.98 V.

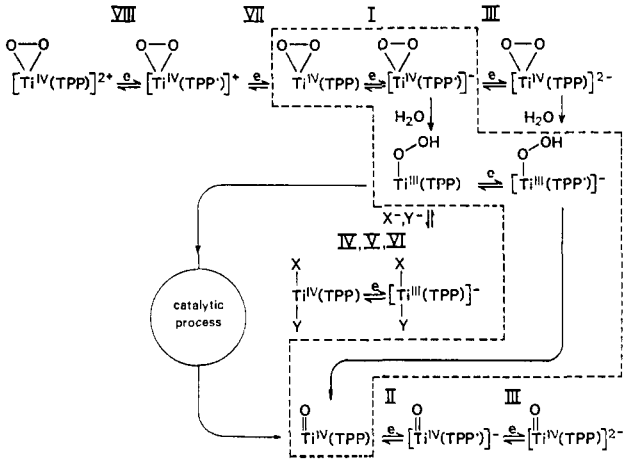

Figure 11. Summary of redox processes for $Ti(O_2)(TPP)$ in CH_2Cl_2 (0.1 M TBAP) solution. The dashed box shows the ECEC mechanism of the reductive cleavage of coordinated peroxide. See text for explanation of the catalytic process. The redox chemistry of $Ti(O_2)(OEP)$ is similar.

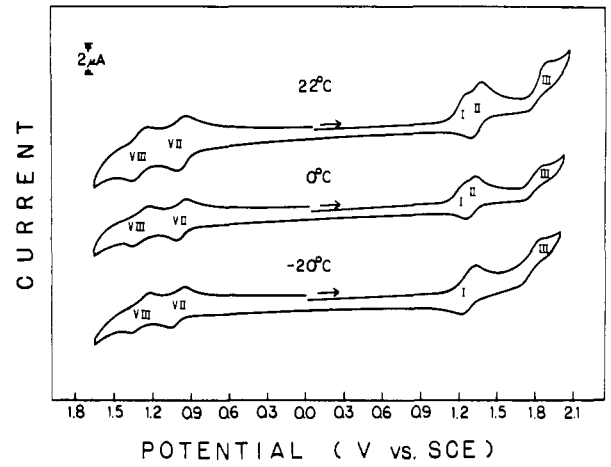

Figure 12. Cyclic voltammograms for 1 mM $Ti(O_2)(OEP)$ in CH_2Cl_2 (0.1 M TBAP) at various temperatures.

limited extent. Possible causes of this substoichiometric reduction are an incomplete reaction with water (eq 9) and/or a slow kinetics of this reaction relative to those of competing processes (vide infra).

Reaction 8 does not appear to be reversible at room temperature because it is followed by chemical and electrochemical steps (reactions 9–11). At low temperature, at short times of electrolysis, or in strictly anhydrous solution, TiO(TPP) is not generated. Therefore, the reaction described by eq 3 does not occur, and wave II is not observed. Both the $[Ti(O_2)(TPP\cdot)]^-$ and $[TiO(TPP\cdot)]^-$ radicals are reduced at approximately the same potential (see Table I) to form the dianions, $[Ti(O_2)(TPP)]^{2-}$ and $[TiO(TPP)]^{2-}$, respectively.

At fast potential scan rates ($v > 500$ mV/s), reaction 11 is not completed and therefore a small wave (wave III′) was observed for reduction of $[Ti^{III}(OOH)(TPP\cdot)]^-$ to the dianion (see Figure 6).

$$[Ti^{III}(OOH)(TPP\cdot)]^- + e^- \rightleftharpoons [Ti^{III}(OOH)(TPP)]^{2-} \quad (14)$$

Also, at high scan rates, waves IV–VI were obtained (Figure 6 and eq 7) and are due to oxidation of various titanium(III) porphyrin complexes derived from $Ti^{III}(OOH)(TPP)$.

The presence of titanium(III) porphyrin species in the reduced solution suggests that additional pathways might contribute to the reduction of the peroxo ligand. It has been shown earlier that $Ti^{IV}(O_2)(TPP)$ is reduced to $Ti^{IV}O(TPP)$ by two molecules of $Ti^{III}F(TPP)$, through the intermediacy of the $Ti^{IV}(O)(F)(TPP\cdot)$ cation radical complex.[21] In a similar fashion, a catalytic mechanism for the two-electron reduction of $Ti^{IV}(O_2)(TPP)$ may be proposed according to reactions 15–19. The overall reaction occurring in this catalytic cycle

$$Ti^{III}(OOH)(TPP) + X^- \rightleftharpoons Ti^{III}X(TPP) + HO_2^- \quad (15)$$

$$Ti^{III}X(TPP) + Ti^{IV}(O_2)(TPP) \rightarrow Ti^{IV}(O)(X)(TPP\cdot) + Ti^{IV}O(TPP) \quad (16)$$

$$Ti^{IV}(O)(X)(TPP\cdot) + Ti^{III}X(TPP) \rightarrow Ti^{IV}O(TPP) + Ti^{IV}X_2(TPP) \quad (17)$$

$$Ti^{IV}X_2(TPP) + e^- \rightleftharpoons [Ti^{III}X_2(TPP)]^- \quad (18)$$

$$[Ti^{III}X_2(TPP)]^- \rightleftharpoons Ti^{III}X(TPP) + X^- \quad (19)$$

is a two-electron reduction of the peroxo ligand of $Ti(O_2)(TPP)$. The formation of TiX(TPP), the catalytically active species, requires the loss of some hydroperoxide ligand according to reaction 15; this might contribute to the substoichiometric character of the peroxo ligand reduction, as noted above. Regeneration of the catalytically active titanium(III) species is very fast, since the half-wave potential of reaction 18 is about 0.5 V more positive than that of reaction 8. A summary of the overall reduction mechanisms of $Ti(O_2)(TPP)$ is shown in Figure 11.

Finally, another process that might occur in this system is an electrochemically induced axial ligand exchange, according to reaction 20. Peroxo ligand substitution probably occurs

$$[Ti^{IV}(O_2)(TPP\cdot)] + H_2O \rightleftharpoons [Ti^{IV}O(TPP\cdot)]^- + H_2O_2 \quad (20)$$

at a faster rate in the anion radical complex than in the parent species. It has been shown that the structurally analogous (catecholato)titanium(IV) tetraphenylporphyrin radical anion complex undergoes axial ligand exchange to give $[Ti^{IV}O(TPP\cdot)]^-$; this process is slow on the cyclic voltammetry time scale but is fully operative during controlled-potential electrolysis.[26] A similar situation probably prevails for the relative kinetics of reactions 8 and 20, with the substoichiometric character of the peroxo ligand reduction as a consequence.

Reduction of $Ti(O_2)(OEP)$. The reduction of $Ti(O_2)(OEP)$ is similar to that observed for $Ti(O_2)(TPP)$. Figure 12 illustrates typical cyclic voltammograms of $Ti(O_2)(OEP)$ in CH_2Cl_2 (0.1 M TBAP) solution. At room temperature three reduction peaks were observed (at −1.18, −1.23, and −1.76 V). The half-wave potentials for the corresponding first and second reductions of $Ti(O_2)(TPP)$ and $Ti(O_2)(OEP)$ differ by 210–190 mV (Table I). These differences are close to the 200-mV value obtained for the two ring reductions of H_2TPP and H_2OEP[20] and indicate that, in the case of $Ti(O_2)(OEP)$, the first two reductions also occur at the conjugated porphyrin ring.

The initial one-electron-transfer reaction at $E_p = -1.18$ V (or $E_{1/2} = -1.25$ V at −20 °C) is due to reduction of $Ti(O_2)(OEP)$ to form an anion radical:

$$Ti(O_2)(OEP) + e^- \rightleftharpoons [Ti(O_2)(OEP\cdot)]^- \quad (21)$$

The ESR spectrum of the solution reduced at −1.20 V had a room- and low-temperature signal with g values ranging from 2.007 to 2.009 (Table III). A small change in this signal was observed after longer times of electrolysis (longer than 80 s), and the final ESR spectrum obtained was identical (in shape) with that obtained for $[TiO(TPP\cdot)]^-$ (see Figure 8b). This suggests that the products of reduction are analogous to those obtained for $Ti(O_2)(TPP)$.

The time-resolved electronic absorption spectra of electrogenerated $[Ti(O_2)(OEP\cdot)]^-$ and $[TiO(OEP\cdot)]^-$ radicals are

(26) Deronzier, A.; Latour, J. M. *Nouv. J. Chim.* **1984**, *8*, 393–399.

Table III. ESR[a] Data for Oxidized and Reduced Titanium(IV) Porphyrins in CH_2Cl_2 (0.1 M TBAP)

	295 K		130 K	
porphyrin	Red(1)	Ox(1)	Red(1)	Ox(1)
TiO(TPP)	2.005	2.004	2.007	2.005
$Ti(O_2)$(TPP)	2.004	2.008	2.010	2.010
$Ti(O_2)$(OEP)	2.007	2.006	2.009	2.007

[a] All g values ±0.001.

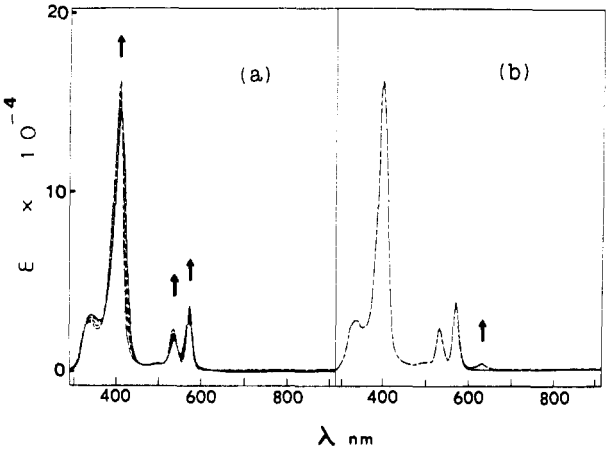

Figure 13. Time-resolved electronic absorption spectra for the reduction of $Ti(O_2)$(OEP) at −1.20 V in CH_2Cl_2 (0.1 M TBAP) (a) after 80 s of electrolysis and (b) after 450 s (2-mm cell).

shown in Figure 13 (wavelengths and molar absorptivities are listed in Table II). In contrast to the spectrum of $[Ti(O_2)(TPP\cdot)]^-$, no characteristic peak for the $[Ti(O_2)(OEP\cdot)]^-$ radical was found in the range of 600–900 nm (Figure 13a). A small peak that is characteristic for $[TiO(OEP\cdot)]^-$ appeared at 632 nm (Figure 13b). Spectral changes during the third reduction could not be obtained due to the proximity of this reaction with the potential limit of the solvent.

The $[Ti(O_2)(OEP\cdot)]^-$ radical is more stable than $[Ti(O_2)(TPP\cdot)]^-$. This was confirmed by cyclic voltammetric measurements at low temperature (Figure 12). At −20 °C step II was not observed. At the same time step I has become completely reversible with a half-wave potential of −1.25 V. This same change with temperature was observed for $Ti(O_2)$(TPP), but at a temperature about 40 °C lower.

Three waves (at $E_{1/2}$ = −0.55, −0.12, and 0.56 V) due to the oxidation of Ti(III) to Ti(IV) were obtained upon reversal of the potential scan after step I. These waves were not observed if the time between the switching potential on the plateau of wave I and the oxidation potential of peak IV was longer than 3 s. This time can be compared to the 4 s needed to see the peaks with $Ti(O_2)$TPP and indicates that the amount of Ti(III) generated during the first reduction step of $Ti(O_2)$(OEP) is smaller than that during the first reduction step of $Ti(O_2)$(TPP). It also provides further proof for the higher stability of $[Ti(O_2)(OEP\cdot)]^-$.

The above spectral data, as well as the similarity between the cyclic voltammetry of $Ti(O_2)$(TPP) and $Ti(O_2)$(OEP), suggest that the actual reduction mechanism of the two compounds in CH_2Cl_2 (0.1 M TBAP) are similar and can be described by the mechanism shown in Figure 11.

Electrochemical Oxidation of TiO(TPP), $Ti(O_2)$(TPP), and $Ti(O_2)$(OEP). In the range of potential between 0.0 and 1.7 V vs. SCE, two well-defined waves were obtained by cyclic voltammetry for $Ti(O_2)$(TPP) and $Ti(O_2)$(OEP) as well as for TiO(TPP). (These peaks are labeled VII and VIII in Figures 1, 6, and 12.) Half-wave potentials for each oxidation step are listed in Table I. The currents observed by cyclic voltammetry for the two steps of each complex are equal in

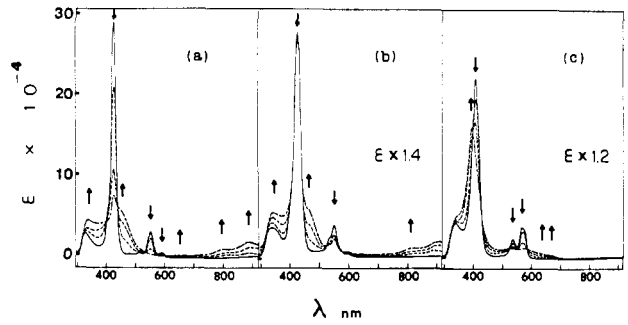

Figure 14. Time-resolved electronic absorption spectra obtained during the first oxidation (reaction VII) of (a) TiO(TPP), (b) $Ti(O_2)$(TPP), and (c) $Ti(O_2)$(OEP) in CH_2Cl_2 (0.1 M TBAP) solution.

height, indicating an identical number of electrons transferred in peak VII and peak VIII. In addition, $E_{pa} - E_{pc} = 60 \pm 5$ mV at low scan rates (v = 100 mV/s), and $i_p/v^{1/2}$ from the cyclic voltammograms was constant for the two processes, indicating that one electron is reversibly transferred in each oxidation.

Confirmation of the overall number of electrons transferred in each step was obtained by controlled-potential electrolysis. Controlled-potential electrolysis of TiO(TPP) at 1.29 V showed a one-electron oxidation as the color changed from pink to yellow-green and finally to green during the second one-electron oxidation at 1.55 V. Controlled-potential electrolysis of $Ti(O_2)$(TPP) at 1.25 V also showed a one-electron oxidation as the color changed from pink to brown and, during the second one-electron step at 1.40 V, to green. Electrolysis of $Ti(O_2)$(OEP) was performed at 1.20 and 1.50 V, and similar color changes were observed. All oxidations were totally reversible on the macroelectrolysis time scale as evidenced by the fact that rereduction of the two-electron-oxidized solutions could be accomplished at a potential 200 mV cathodic of the first oxidation with the addition of two electrons and produced solutions that showed the original colors and spectra.

As seen in Table I, there is no significant difference in potential for the first oxidation of TiO(TPP) and $Ti(O_2)$(TPP). However, the presence of a peroxo group in $Ti(O_2)$(TPP) changes the potential of the second oxidation, which is 100 mV more negative than that observed for TiO(TPP). The half-wave potential of the first oxidation of $Ti(O_2)$(TPP) is 150 mV more positive than that for $Ti(O_2)$(OEP). This is reasonable since the first oxidation potentials of H_2TPP and H_2OEP also differ by 150 mV (0.96 and 0.81 V, respectively).

The peak separation between the first oxidation (wave VII) and the first reduction (wave II) for TiO(TPP) and the peroxo compounds ranged from 2.23 to 2.27 V, suggesting that all reactions are porphyrin-ring based.[20] However, another commonly used test for differentiating a porphyrin-ring oxidation from a metal-center oxidation is the potential difference between the two oxidations.[20] The experimental values indicate some deviation from the expected value of 0.29 ± 0.05 V for TiO(TPP) and $Ti(O_2)$(TPP) but not for $Ti(O_2)$(OEP). This deviation is especially large in $Ti(O_2)$(TPP). Also, the values of $E_{1/2}$[Ox(2) − Ox(1)] measured for each investigated compound in CH_2Cl_2 (0.1 M TBAP) are about 100 mV lower than those measured in CH_2Cl_2 (0.1 M $TBAPF_6$). This is probably due to a surface effect similar to that observed for electrooxidation of various Ni(II) tetraphenylporphyrins and tetraphenylchlorin complexes in CH_2Cl_2 with TBAP or $TBAPF_6$ as supporting electrolyte.[27]

Spectra associated with each oxidation step are illustrated in Figures 14 and 15 and the molar absorptivities of the major

(27) Chang, D.; Malinski, T.; Ulman, A.; Kadish, K. M. *Inorg. Chem.* **1984**, *23*, 817–824.

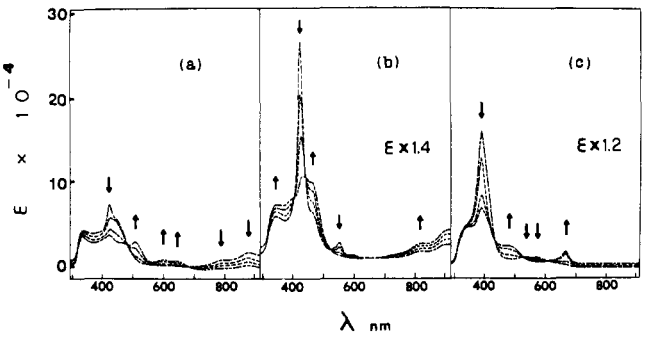

Figure 15. Time-resolved electronic absorption spectra obtained during the second oxidation (reaction VIII) of (a) TiO(TPP), (b) Ti(O_2)(TPP), and (c) Ti(O_2)(OEP) in CH_2Cl_2 (0.1 M TBAP) solution.

peaks summarized in Table II. During the first oxidation of TiO(TPP) and Ti(O_2)(TPP) both the Soret and Q bands decreased in intensity. At the same time, new bands were formed at about 800 and 900 nm, indicating radical cation formation. The intensity of the Soret band during the electrolysis of Ti(O_2)(OEP) also decreased significantly and was shifted to shorter wavelengths. The Q bands almost completely disappeared, and two new small bands between 600 and 700 nm were formed, also indicating cation radical formation.

The ESR spectra recorded after the first oxidation step are very consistent with the electrochemical and spectroelectrochemical data and show isotropic signals with g values ranging from 2.004 to 2.008. These values are listed in Table III. When the temperature was lowered to 130 K, no color change was observed for the frozen solids, which had similar isotropic ESR signals with g values from 2.005 to 2.010 (Table III). The second oxidation of TiO(TPP), Ti(O_2)(TPP), or Ti(O_2)(OEP) produced green solutions in all cases, whose UV–visible spectra were similar to those of the $[Zn^{II}(TPP)]^{2+}$ and $[Mg^{II}(OEP)]^{2+}$ dications.[17] No ESR signals were detected at this point.

The above spectral data, as well as the similarity in the cyclic voltammetry of TiO(TPP), Ti(O_2)(TPP), and Ti(O_2)(OEP), suggest that the oxidation mechanism of these three compounds in CH_2Cl_2 (0.1 M TBAP) are similar and can be described as shown in reaction 22. In this reaction n = 1 where P = TPP and n = 2 where P = TPP or OEP.

$$[Ti^{IV}(O_n)(P)]^{2+} \overset{\text{VIII}}{\rightleftharpoons} [Ti^{IV}(O_n)(P^{\bullet})]^{+} \overset{\text{VII}}{\rightleftharpoons} Ti^{IV}(O_n)(P) \quad (22)$$

Conclusion

In this study the electrochemistry and spectroelectrochemistry of oxo- and peroxotitanium(IV) porphyrin complexes have been characterized. In addition, new spectral data for the oxidized forms of Ti(O_2)(TPP) and Ti(O_2)(OEP) and for the $[Ti(O_2)(TPP^{\bullet})]^-$ and $[Ti(O_2)(OEP^{\bullet})]^-$ anion radicals are presented. An ECEC reduction mechanism is proposed for the two-electron reduction of the coordinated peroxide in Ti(O_2)(TPP) and Ti(O_2)(OEP). The first step of this mechanism is a one-electron-transfer reaction that occurs on the porphyrin ring. Although the mechanisms for the oxidation and reduction of Ti(O_2)(TPP) and Ti(O_2)(OEP) are virtually identical, it must be noted that a clear difference does exist in the stability of the electrochemically generated radicals.

Acknowledgment. The support of the National Science Foundation (K.M.K., Grant CHE 8215507) and of the Centre National de la Recherche Scientifique (LA 321 and ERA 468) are gratefully acknowledged. M.G. and K.M.K. also acknowledge support from NATO, Scientific Affairs Division (Grant R.G.095-82).

Registry No. TiO(TPP), 58384-89-7; Ti(O_2)(TPP), 65651-28-7; Ti(O_2)(OEP), 60217-35-8; $[TiO(TPP^{\bullet})]^-$, 92186-11-3; $[TiO(TPP)]^{2-}$, 92186-12-4; $[Ti(O_2)(TPP^{\bullet})]^-$, 92186-13-5; $[Ti(O_2)(TPP)]^{2-}$, 92186-14-6; $[Ti(O_2)(OEP^{\bullet})]^-$, 92186-15-7; $[TiO(OEP^{\bullet})]^-$, 92186-16-8; $[Ti^{IV}(O)(TPP^{\bullet})]^+$, 92186-17-9; $[Ti^{IV}(O_2)(TPP^{\bullet})]^+$, 92186-18-0; $[Ti^{IV}(O_2)(OEP^{\bullet})]^+$, 92186-19-1; $[Ti^{IV}(O)(TPP)]^{2+}$, 92186-20-4; $[Ti^{IV}(O_2)(TPP)]^{2+}$, 92186-21-5; $[Ti^{IV}(O_2)(OEP)]^{2+}$, 92186-22-6; sodium anthracenide, 12261-48-2; oxygen, 7782-44-7.